Inorganica Chimica Acta, *95* (1984) 29–35

Optical and Magnetic Properties of Uranium and Neptunium Borohydrides and Tetrakismethylborohydrides

K. RAJNAK†, E. GAMP, R. BANKS, R. SHINOMOTO and N. EDELSTEIN*

Materials and Molecular Research Division, Lawrence Berkeley Laboratory, University of California, Berkeley, Calif. 94720, U.S.A.

Received October 5, 1983

Magnetic susceptibilities of the compounds $U(BH_3CH_3)_4$ *and* $Np(BH_3CH_3)_4$ *are reported in the temperature range 2 K–330 K. With this additional data, the optical spectrum of* $U(BD_4)_4$ *diluted in* $Hf(BD_4)_4$ *is reanalyzed. Preliminary results are also given for the analysis of the optical spectrum of* $Np(BD_4)_4$ *diluted in* $Zr(BD_4)_4$*. Electron paramagnetic resonance data are presented for single crystals of* $Np(BH_3CH_3)_4$ *diluted in* $Zr(BH_3CH_3)_4$*.*

Introduction

The actinide borohydrides possess a number of properties which make them attractive candidates for chemical and spectroscopic studies. The first five members of the series (Th–Pu) have been prepared [1–3]. They are volatile molecules near room temperature which makes it relatively easy to obtain single crystals. High symmetry diamagnetic analogs, Hf or Zr borohydride, are available as diluents [4, 5]. In a pioneering study, Bernstein and Keiderling [6] (BK) obtained high resolution optical spectra of $U(BH_4)_4(U(BD_4)_4)$ in single crystals of $Hf(BH_4)_4$-$(Hf(BD_4)_4)$ and fit this data to a parameterized Hamiltonian which included the Slater parameters, the spin–orbit coupling constant, and two crystal field parameters reflecting the T_d symmetry of the host crystals. Subsequently, the molecules Np and Pu borohydride were synthesized and $Np(BH_4)_4(Np(BD_4)_4)$ diluted in $Zr(BH_4)_4(Zr(BD_4)_4)$ have been the subject of magnetic and spectroscopic investigations [7, 8].

The actinide borohydrides exhibit two structural types. Th, Pa, and $U(BH_4)_4$ are isomorphic and increase in volatility with increasing atomic number. Np and $Pu(BH_4)_4$ are also isomorphic but closely resemble the highly volatile Zr and Hf borohydrides in structure and properties rather than the earlier actinide molecules [9]. All seven compounds contain triple hydrogen bridge bonds connecting the boron atom to the metal. In addition, the 14 coordinate Th, Pa, and U borohydrides have double-bridged borohydride groups that link metal atoms together in a low symmetry, polymeric structure [10]. The structures of the other four molecules are monomeric and much more symmetric, the 12 coordinate metal is surrounded by a tetrahedral array of BH_4^- groups.

The polymeric structure of $U(BH_4)_4$ precludes the possibility of obtaining the magnetic susceptibility of this compound with the same symmetry as found in the host $Hf(BH_4)_4$ crystal used in the optical investigations. However the series of compounds $M(BH_3CH_3)_4$ (M = Th, U, Np, and Zr) have recently been synthesized and structurally characterized [11]. All four molecules are monomeric and for each molecule the metal atom is tetrahedrally coordinated to the four methylborohydride groups through tridentate hydrogen bridge bonds. The Zr and Np tetrakismethylborohydrides belong to the same tetragonal space group with 2 molecules per unit cell. The U and Th compounds are monoclinic and triclinic respectively with 4 molecules per unit cell.

In the following discussion we assume the electronic structures of $M(BH_4)_4$ (for T_d symmetry) and $M(BH_3CH_3)_4$ (M = U or Np) are similar so that we can use the data from one system for the analysis of the other.

The magnetic susceptibilities of $U(BH_3CH_3)_4$ and $Np(BH_3CH_3)_4$ have been measured in the temperature range 2 K–330 K. With this additional information concerning the ground state and the low-lying excited states for the tetragonal $U(BD_4)_4$ systems, the optical data of BK have been reanalyzed. The same procedure has been applied to the optical data for $Np(BD_4)_4$ diluted in $Zr(BD_4)_4$ and the magnetic data for $Np(BH_3CH_3)_4$. Electron paramagnetic resonance (EPR) has also been obtained for $Np(BH_3CH_3)_4$ diluted in $Zr(BH_3CH_3)_4$ and compared with similar data for $Np(BH_4)_4(Np(BD_4)_4)$ diluted in $Zr(BH_4)_4(Zr(BD_4))$ [9]. These topics will be reviewed in this paper.

---

*Author to whom correspondence should be addressed.

†Permanent address: Department of Physics, Kalamazoo College, Kalamazoo, Mich. 49007.

0020-1693/84/$3.00

Experimental

The syntheses of $U(BH_3CH_3)_4$, $Np(BH_3CH_3)_4$, $Zr(BH_3CH_3)_4$, and $Np(BH_4)_4(Np(BD_4)_4)$ have been described previously [3, 11]. Magnetic susceptibility measurements were carried out on a SHE 905 SQUID magnetometer. Powdered samples of $U(BH_3CH_3)_4$ and $Np(BH_3CH_3)_4$ were weighed and sealed into calibrated containers in an inert atmosphere box. For $U(BH_3CH_3)_4$, several different samples were measured with weights varying from 75 to 130 mg. Only one sample of $Np(BH_3CH_3)_4$ was measured with a nominal weight of 10 mg. Because of the problems of obtaining an accurate weight on this small, radioactive sample, the weight of the sample was adjusted so that the susceptibilities at low temperatures agreed with the values calculated from the g value obtained by EPR measurements. All data were obtained with applied fields between 0.5 and 40 kGauss and temperatures from 1.8 to 330 K.

Single crystals of $Np(BH_3CH_3)_4$ diluted in $Zr(BH_3CH_3)_4$ were grown by first adding approximately 1 mg of $Np(BH_3CH_3)_4$ to 50 mg $Zr(BH_3CH_3)_4$ in a pyrex tube in an inert atmosphere box. This tube was removed from the box and evacuated down to 10^{-4} Torr using an oil diffusion pump, and then sealed off under vacuum. Single crystals were obtained by vapor deposition in the upper half of the tube upon heating the lower half at approximately 30 °C. These crystals were oriented for EPR measurements by X-ray identification of the faces and edges of the crystals. EPR spectra at 35 GHz were obtained using a Varian E-110 microwave bridge. The magnetic field was produced by an electromagnet with a 2 inch gap which could be rotated about the vertical axis. The maximum field which could be obtained was approximately 16 kGauss. All samples were run at ~2 K.

Optical spectra have been obtained from the near infra-red region through the visible region on a Cary 17 spectrophotometer. Single crystals of $Np(BH_4)_4$ or $Np(BD_4)_4$ (approximate dimensions 1 cm × 2 cm × 25 microns) were grown by simply cooling the liquid borohydrides very slowly in a quartz sample holder of the above dimensions in the optical dewar. When the sample temperature reached ~150 K in about 8 hours, liquid helium was added and the spectra were recorded at approximately 2 K. Mixed crystals of $Np(BH_4)_4/Zr(BH_4)_4$ or $Np(BD_4)_4/Zr(BD_4)_4$ were grown from the vapor according to the method of BK [8].

$U(BH_4)_4$ and $U(BH_3CH_3)_4$

Review and Magnetic Susceptibility Data

The U^{4+} ion in $U(BH_4)_4/Hf(BH_4)_4$ and $U(BH_3CH_3)_4$ is at a site of T_d symmetry. The ground term of the U^{4+} ion has J = 4 (nominally $^3H_4$) which will split in a tetrahedral crystal field into four states, a singlet A_1, a doublet E and two triplets, T_1 and T_2. BK found no EPR spectra for $U(BD_4)_4/Hf(BD_4)_4$ at 2 or 77 K nor any Zeeman splitting in the 4000–7500 Å region. This fact plus the assignment of at least 11 forced electric dipole transitions led them empirically to assign the ground state as the E state. Their analysis of the optical spectra resulted in a calculated ground state of T_2 symmetry with the E state 14 cm^{-1} above it.

The T_d symmetry about the U^{4+} in $U(BH_3CH_3)_4$ allows us to use magnetic susceptibility measurements from 2 K to room temperature to supplement the data of BK. We assume the electronic structure of $U(BH_3CH_3)_4$ and $U(BH_4)_4$ are similar. The optical spectra of $U(BH_4)_4$ and $U(BH_3CH_3)_4$ obtained in C_6D_6 at room temperature are shown in Fig. 1. As seen from Fig. 1 the spectra are similar, although most bands appear to be shifted to higher energies for $U(BH_3CH_3)_4$. The susceptibility of $U(BH_3CH_3)_4$ is shown in Fig. 2. The ground state shows temperature independent paramagnetism consistent with the assignment of the E state as the ground state. This data was initially analyzed considering only the $^3H_4$ term. Several fits are shown in Fig. 2 with the splittings given in Table I. From these fits it is clear that the splitting between the ground E state and the first excited T_1 or T_2 state must be on the order of or greater than 150 cm^{-1}. Finally it should be noted that a reasonable fit could not be obtained without the introduction of an orbital reduction factor [12].

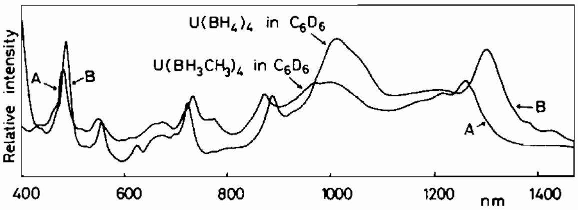

Fig. 1. Optical absorption spectra of $U(BH_4)_4$ and $U(BH_3CH_3)_4$ in C_6D_6 at room temperature.

TABLE I. $U(BH_3CH_3)_4$ Parameters and Energy Levels for Fits Considering only the $^3H_4$ Ground Term.

	A[a]	B[a]
B_0^4 (cm^{-1})	−4442	2473
B_0^6 (cm^{-1})	−2186	−1410
k	0.79	0.79
Energies (cm^{-1})	0 E	0 E
	148 T_2	270 T_1
	875 T_1	648 A_1
	2099 A_1	978 T_2

[a] As in Fig. 2.

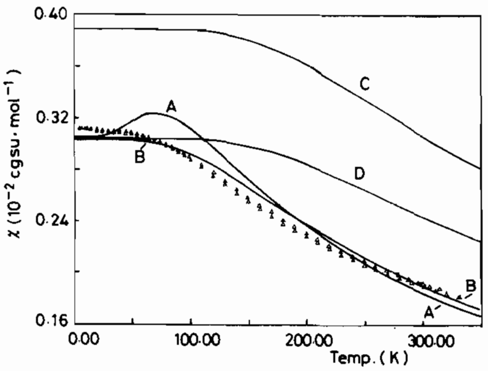

Fig. 2. Paramagnetic susceptibility of $U(BH_3CH_3)_4$. △△, Experimental data obtained at 5 and 40 kGauss; A, B, calculated considering only $^3H_4$ splittings as in Table I; C, calculated from the parameters of a preliminary optical analysis; D, same as C, but with an orbital reduction factor k = 0.93.

Optical Analysis

The energy levels within an f^n configuration in T_d symmetry can be written in terms of the atomic free ion (H_{FI}) and crystal field (H_{CF}) Hamiltonians as follows [13, 14]:

$$H = H_{FI} + H_{CF}$$

where

$$H_{FI} = \sum_{k=0,2,4,6} F^k(nf,nf)f_k + \zeta_f a_{so} + \alpha L(L+1)$$

$$+ \beta G(G_2) + \gamma(R_7) + \sum_{k=0,2,4} m_k M^k + \sum_{k=2,4,6} p_k P^k$$

and

$$H_{CF} = B_0{}^4[C_0{}^{(4)} + \sqrt{5/14}(C_{-4}{}^{(4)} + C_4{}^{(4)})] +$$

$$+ B_0{}^6[C_0{}^{(6)} - \sqrt{7/2}(C_{-4}{}^{(6)} + C_4{}^{(6)})].$$

The $F^k(nf,nf)$'s and ζ_f represent, respectively, the radial parts of the electrostatic and spin–orbit interactions between f electrons, while f_k and a_{so} are the angular parts of the interactions. α, β, and γ are the parameters associated with the two-body effective operators of configuration interaction. The M^k parameters represent the spin-spin and spin–other–orbit interactions while the P^k parameters arise from electrostatic-spin–orbit interactions with higher configurations. The crystal field interaction for T_d symmetry is represented by two parameters $B_0{}^4$ and $B_0{}^6$ and the tensor operators $C_q{}^{(k)}$ [14].

BK used a parameterized Hamiltonian which included only the F^k, ζ, $B_0{}^4$, and $B_0{}^6$. Their best fit for $U(BD_4)_4/Hf(BD_4)_4$ assigned 11 levels with an rms deviation of 62 cm⁻¹ between experimental and calculated levels. However their calculated ground state was a T_2 level with the E level lying 14 cm⁻¹ higher in contradiction with experiment. Furthermore when they assigned 18 energies, their rms deviation increased to 158 cm⁻¹.

Recently, the U^{4+} free-ion spectrum has been completely analyzed [15–17]. With this additional information it is now possible to set certain limits for the allowable range of both the free-ion parameters and their ratios. In addition, 26 levels of $U^{4+}/ThBr_4$ have been fit [18] with an rms deviation of only 36 cm⁻¹, thus providing some guidelines for the changes in the free-ion parameters in going from the free ion to the crystal. From assignments of the infra-red and Raman spectra of $Np(BH_4)_4(Np(BD_4)_4)$, a normal coordinate analysis of these molecules has been carried out [19], which has resulted in a reliable list of frequencies with which to assign vibronic bands in the optical spectrum of $U(BD_4)_4/Hf(BD_4)_4$. For these reasons a reanalysis of the data of BK has been undertaken.

The values of F^2 obtained by BK were 42008 and 1910 cm⁻¹ respectively. The corresponding free-ion parameters have recently been determined as 51938 and 1968 cm⁻¹. The observed reduction in F^2 to 81 percent of the free-ion value is similar to that found for some Cr^{3+} compounds [20], but the decrease in ζ of only 3 percent seems very small by comparison. In the reanalysis we initially assumed that the ratios F^4/F^2 and F^6/F^2 should lie somewhere between their free ion values (0.82 and 0.53) and their values for $U^{4+}/ThBr_4$ (0.96 and 0.64). We further assumed that the values of F^2 and ζ should be reduced from the free-ion values in the same ratio as found for $U^{4+}/ThBr_4$. Initial values of α, β, γ, M^ks, and P^ks were taken from the $U^{4+}/ThBr_4$ analysis. Even though the sparseness of the data does not allow a determination of all these parameters, it is important to include them at reasonable values. The distortion of the calculated level scheme due to errors of 20–30 percent in the values of these parameters is less than that caused by setting them equal to zero. This is particularly important for the tetravalent actinides because the spin–orbit coupling and crystal field interactions are both large. The states are so mixed that a number of different sets of parameters will produce moderately good fits (rms deviation ~100 cm⁻¹). Only a very good fit that allows further assignments of missing levels can guarantee a unique set of parameters. Finally, in our reanalysis we took account of the magnetic susceptibility data by forcing the first excited state to be greater than 150 cm⁻¹ above the ground E state.

With the above assumptions it was immediately obvious that some of BK's uncertain origins could not be fit with our parameter values. Two of the original 11 levels have been reassigned and we kept only three of the less certain ones. The seven new assignments were verified by the identification of vibronic bands based on the electronic origins. Vibronic lines based on origins we discarded have been reassigned. Our final fit induced all 19 of the allowed transitions

TABLE II. Parameter Values[a] (cm^{-1}) for U^{4+}.

	$U(BD_4)_4$ in $Hf(BD_4)_4$		U^{4+}: $ThBr_4$[b]	Free Ion[c]
	BK	This work		
F^2	42008	41121(236)	42253(127)	51938 ± 39
F^4	37679	38849(1071)	40458(489)	42708 ± 100
F^6	28048	21711(827)	25881(383)	27748 ± 68
F^4/F^2	0.90	0.94	0.96	0.82
F^6/F^2	0.67	0.53	0.61	0.53
α	–	40(3)	31(1)	33.5 ± 0.4
β	–	[–648]	–644(75)	–664 ± 25
γ	–	[1200]	[1200]	744 ± 26
ζ	1910.8	1807(16)	1783(7)	1968 ± 2
P^2	–	[500]	[500]	573 ± 66
P^4	–	[500]	[500]	524 ± 144
P^6	–	[500]	[500]	1173 ± 321
$B_0{}^4$	–3484	–2486(170)	1316(146)	
$B_0{}^6$	–4240	–5287(113)	–3170(379)	
$B_4{}^4$	–	–	–2230(85)	
$B_4{}^6$	–	–	686(246)	
$B_0{}^2$	–	–	–1096(80)	
Number Levels	11	19	26	13
σ	62	71	36	9.8

[a] Parameters in [ ] were held fixed. In all cases $M^0 = 0.987$, $M^2 = 0.550$, $M^4 = 0.384$. [b] Reference [18]. [c] Reference [15].

(selection rules E → T_1, T_2) with an rms deviation of 71 cm^{-1}. The parameter values for this fit are given in Table II along with those of BK and for U^{4+}/$ThBr_4$, and the U^{4+} free ion. The detailed analysis will appear in a forthcoming publication [21]. It is interesting to note that our crystal field parameters are not much different than for those of BK, $B_0{}^4$ is somewhat smaller while $B_0{}^6$ is somewhat larger. It is the free-ion parameters that have been markedly changed and which are now more consistent with other available U^{4+} data.

The magnetic susceptibility, χ, has been calculated from the above parameters and is also shown in Fig. 2. The calculated values of χ are too large and the introduction of an orbital reduction factor k = 0.93 gave a better fit, which is also shown in Fig. 2. As will be shown later, this parameter is also necessary for the $Np(BH_4)_4$ molecule.

$Np(BH_4)_4$ and $Np(BH_3CH_3)_4$

Magnetic and Optical Data

The EPR data for $Np(BD_4)_4/Zr(BD_4)_4$ and $Np(BH_3CH_3)_4/Zr(BH_3CH_3)_4$ can be summarized in terms of the parameters of a spin-Hamiltonian [22]

$$H = \beta H(g_xH_xS_x + g_yH_yS_y + g_zH_zS_z) + A_xS_xI_x + A_yS_yI_y + A_zS_zI_z$$

TABLE III. Spin Hamiltonian Parameters for ^{237}Np: $Zr(H_3B{-}R)_4$.

Host	$Zr(H_3B{-}H)_4$	$Zr(H_3B{-}CH_3)_4$
g_x	1.894(2)	1.7739(4)
g_y		1.8292(4)
g_z		1.7961(5)
$A_x(cm^{-1})$	0.1140(10)	0.1079(2)
$A_y(cm^{-1})$		0.1153(2)
$A_z(cm^{-1})$		0.1135(2)
g_{ave}	1.894	1.7997(4)
$A_{ave}(cm^{-1})$	0.1140	0.1122(2)

where the effective spin S = 1/2, the nuclear spin I = 5/2; β is the Bohr magneton; g_k, A_k, k = x, y, z; are the principal axes of the g and A tensors. The values are given in Table III. The resonance spectrum from $Np(BD_4)_4$ is isotropic ($g_x = g_y = g_z$, $A_x = A_y = A_z$) while that from $Np(BH_3CH_3)_4$ is slightly anisotropic. A model to explain this anisotropy will be discussed later. The magnitude of the g value for $Np(BH_4)_4$-($Np(BD_4)_4$) is 1.894 while the average value for $Np(BH_3CH_3)_4$ is 1.800. The susceptibility of $Np(BH_3CH_3)_4$ is shown in Fig. 3.

The ground term for an f^3 system is a J = 9/2 (nominally $^4I_{9/2}$) which will split in T_d crystal field into a doubly degenerate Γ_6 state and two quadruply degenerate Γ_8 states. Only the Γ_6 state will give an

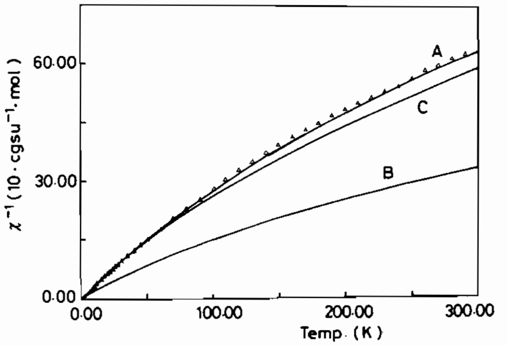

Fig. 3. Inverse paramagnetic susceptibility of $Np(BH_3CH_3)_4$. △△, Experimental data obtained at 5 kGauss; A, calculated considering only $^4I_{9/2}$, $B_0^4 = -1461$ cm^{-1}, $B_0^6 = -3274$ cm^{-1}, orbital reduction factor k = 0.82; B, calculated from the parameters of a preliminary optical analysis; C, same as B with an orbital reduction factor k = 0.87.

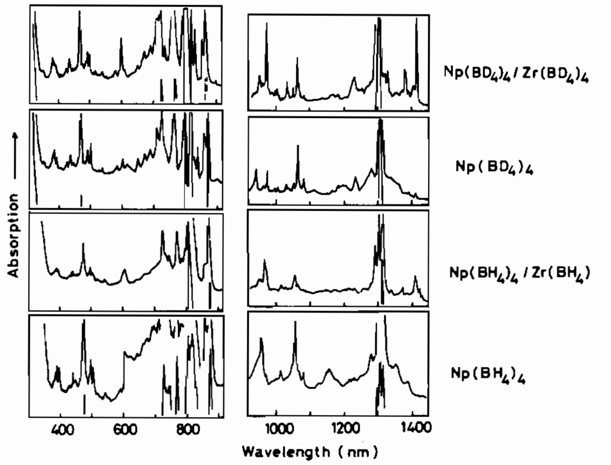

Fig. 4. Optical absorption spectrum of $Np(BH_4)_4$ and $Np(BD_4)_4$, single crystals at 2 K.

isotropic g value so that we can assign the observed EPR spectrum to a Γ_6 ground state.

Part of the optical spectra of $Np(BH_4)_4$ is shown in Fig.4. Unfortunately, there are no reliable free-ion or crystal data for Np^{4+} from which we can obtain reasonable starting parameters. However the low lying energy levels (below 10000 cm^{-1}) are reasonably well separated and can be assigned on the basis of parameters extrapolated from $U(BD_4)_4/Hf(BD_4)_4$ and fixed ratios of F^4/F^2 and F^6/F^2. Starting from this basis a number of further assignments can be made. In a preliminary analysis we assigned 30 levels which could be fit with an rms deviation between the calculated and experimental energies of 83 cm^{-1}. In contrast with the U^{4+} case, we found $B_0^4 \sim B_0^6 \sim -5000$ cm^{-1}. But, by changing the identification of some of the origins in the infra-red region, we were eventually able to fit 46 levels with $\sigma = 84$ cm^{-1} and crystal field parameters very similar to those for $U(BD_4)_4$ [23].

Considering only the $^4I_{9/2}$ ground term the magnetic susceptibility of $Np(BH_3CH_3)_4$ was calculated as a function of temperature. This curve is labelled A in Fig. 3. In order to obtain this curve an orbital reduction factor of 0.82 was needed. The optical analysis described above yielded a g value for the ground Γ_6 state of 2.3 and the magnetic susceptibility calculated from the intermediate coupled wavefunction obtained from the preliminary analysis without an orbital reduction factor gave curve B in Fig. 3. Inclusion of an orbital reduction factor of 0.87 in this calculation gave curve C.

Anisotropic Magnetic Properties of $Np(BH_3CH_3)_4/Zr(BH_3CH_3)_4$

The single crystal EPR spectrum of $Np(BH_3CH_3)_4/Zr(BH_3CH_3)_4$ clearly indicates the presence of two inequivalent sites (see Fig. 5) in the $Zr(BH_3CH_3)_4$ at 2 K. By following the EPR spectrum as a function of the angle of the magnetic field with respect to the crystal axes, the principal axes of the g and A tensors may be determined. The change in the resonance field with magnet rotation angle in the plane perpendicular to the *c* axis is shown in Fig. 6.

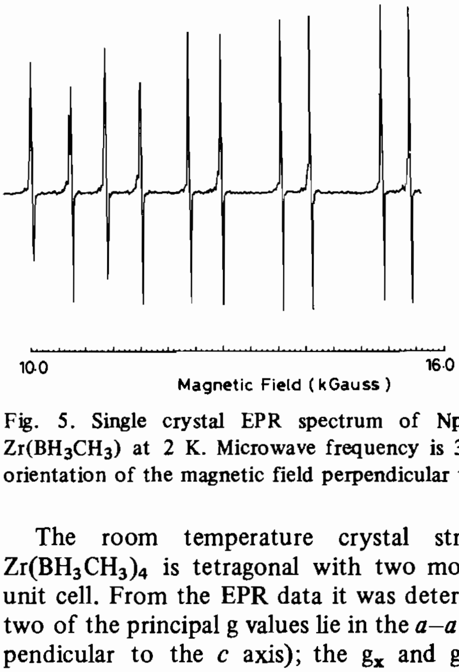

Fig. 5. Single crystal EPR spectrum of $Np(BH_3CH_3)_4/Zr(BH_3CH_3)$ at 2 K. Microwave frequency is 34.700 GHz, orientation of the magnetic field perpendicular to the *c* axis.

The room temperature crystal structure of $Zr(BH_3CH_3)_4$ is tetragonal with two molecules per unit cell. From the EPR data it was determined that two of the principal g values lie in the *a–a* plane (perpendicular to the *c* axis); the g_x and g_y axes are parallel to the projections of the Zr–B bonds on the *a–a* plane. The g_x and g_y axes of the first molecule in the unit cell are rotated by 90° with respect to those of the second molecule. This is shown in Fig. 7. The g_z axis for both molecules is parallel to the *c* axis of the unit cell.

The room temperature crystal structure of $Zr(BH_3CH_3)_4$ shows the two molecules per unit cell are structurally equivalent within the standard deviations of the bond distances and angles. It is

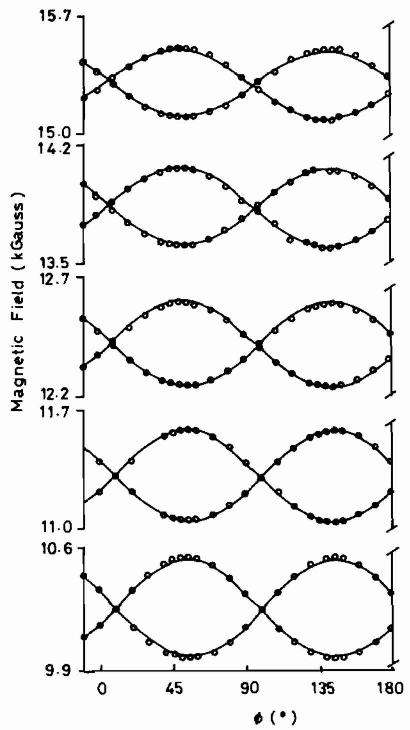

Fig. 6. $Np(BH_3CH_3)_4/Zr(BH_3CH_3)_4$, angular dependence of resonance fields in the *a–a* plane; ϕ is the angle of the magnetic field with the crystallographic (110) plane. Solid lines were calculated from the parameters in Table III.

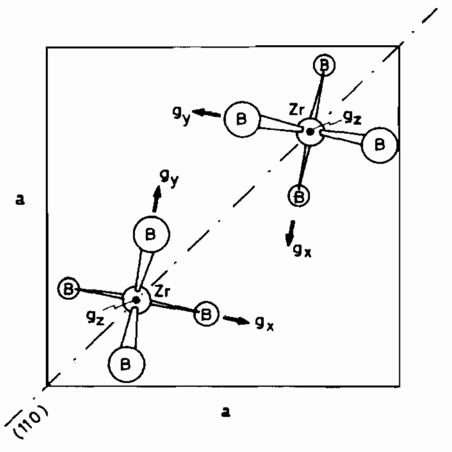

Fig. 7. $Np(BH_3CH_3)_4/Zr(BH_3CH_3)_4$, orientation of the g-tensor axes in the crystallographic unit cell. The view is along the *c* axis, the Zr(Np) atoms are located at (0.25, 0.25, 0.25) and (0.75, 0.75, 0.75).

possible that the crystal undergoes a phase transition on cooling from room temperature to 2 K or upon the inclusion of the impurity $Np(BH_3CH_3)_4$. In order to obtain an idea of the sensitivity of the g value to the geometry of $Np(BH_3CH_3)_4$ we performed the following calculation. First we arbitrarily determined a set of crystal field parameters which would give the correct ground state g value assuming T_d symmetry. Using these parameters, the point charge model [24], and the bond lengths and angles determined from the X-ray structure, we calculated the charge q in the point charge model. We then introduced a distortion by increasing the angle between the Np-H bonds and the *c*-axis by an angle δ thus reducing the symmetry from T_d to D_{2d}. Using the empirically determined q, we recalculated new crystal field parameters from the point charge model. These yielded a new wavefunction from which $g_\parallel$ and $g_\perp$ were calculated. The changes in the g values and in the splitting of the first Γ_8 state *vs.* the distortion angle δ are shown in Fig. 8.

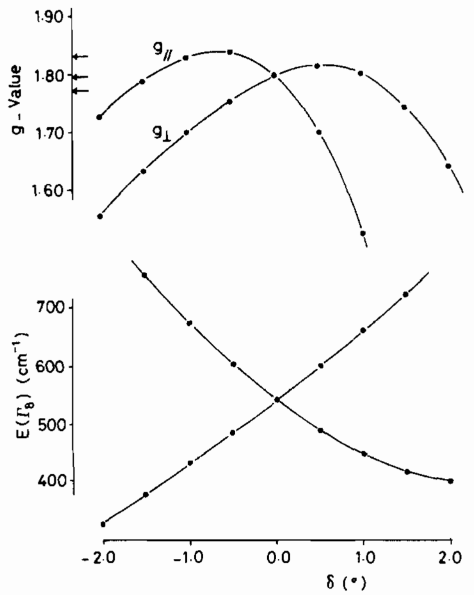

Fig. 8. Influence of an axial distortion on the g-value and the energy of the lowest Γ_8 state. The arrows indicate the experimental g values.

A distortion of approximately 0.5 degrees (within the error limits of the X-ray structure analysis) is enough to account for the observed anisotropy. A similar result was obtained for a rhombohedral distortion model. This approximate calculation suggests that g value anisotropy is a sensitive probe of small structural distortions.

Summary

The optical and magnetic properties of $M(BH_3R)_4$ (M = U, Np; R = H, CH_3) have been determined and the data fit with the parameters of an empirical Hamiltonian. Reasonable fits to the optical data are obtained, but in order to fit the magnetic susceptibility and EPR data, orbital reduction factors of ~0.8–0.9 must be used.

Acknowledgements

This work was supported by the Director, Office of Energy Research, Office of Basic Energy Sciences, Chemical Sciences Division of the U.S. Department of Energy under Contract No. DE-AC03-76SF00098.

References

1 H. I. Schlesinger and H. C. Brown, *J. Am. Chem. Soc., 75,* 219 (1953).

2 H. R. Hoekstra and J. J. Katz, *J. Am. Chem. Soc., 71,* 2488 (1949).

3 R. H. Banks, N. M. Edelstein, R. R. Rietz, D. H. Templeton and A. Zalkin, *J. Am. Chem. Soc., 100,* 1975 (1978).

4 W. E. Reid Jr., J. M. Bish and A. Brenner, *J. Electrochem. Soc., 104,* 21 (1957).

5 B. D. James, R. K. Nanda and M. G. H. Wallbridge, *J. Chem. Soc. (A),* 182 (1966).

6 E. R. Bernstein and T. A. Keiderling, *J. Chem. Phys., 59,* 2105 (1973). This paper will be referred to as BK.

7 R. H. Banks and N. M. Edelstein. in 'Lanthanide and Actinide Chemistry and Spectroscopy', N. Edelstein, (ed.) ACS Symposium Series 131, Washington, D. C., 1980, p. 331. When the text refers to both the hydrogenated and deuterated species, the deuterated molecule is given in parentheses.

8 R. H. Banks, *Ph.D. Thesis,* LBL-10292, 1979.

9 R. H. Banks, N. M. Edelstein, B. Spencer, D. H. Templeton and A. Zalkin, *J. Am. Chem. Soc., 102,* 620 (1980).

10 E. R. Bernstein, W. C. Hamilton, T. A. Keiderling, S. J. LaPlaca, S. J. Lippard and J. J. Mayerle, *Inorg. Chem., 11,* 3009 (1972).

11 R. Shinomoto, E. Gamp, N. M. Edelstein, D. H. Templeton and A. Zalkin, *Inorg. Chem., 22,* 2351 (1983).

12 J. Owen and J. H. M. Thornley, *Repts. Prog. Phys., 29,* 675 (1966).

13 W. T. Carnall, H. Crosswhite, H. M. Crosswhite, J. P. Hessler, N. M. Edelstein, J. G. Conway, G. V. Shalimoff and R. Sarap, *J. Chem. Phys., 72,* 5089 (1980).

14 B. G. Wybourne, 'Spectroscopic Properties of Rare Earths', John Wiley and Sons, Inc., New York, 1965. Our definition for the crystal field parameters follows Wybourne's convention.

15 C. H. H. Van Deurzen, K. Rajnak and J. G. Conway, *J. Opt. Soc. Amer. B, 1,* 45 (1984).

16 J. F. Wyart, V. Kaufman and J. Sugar, *Physica Scripta, 22,* 389 (1980).

17 Z. B. Goldschmidt, *Phys. Rev. A., 27,* 740 (1983).

18 P. Delamoye, K. Rajnak, N. M. Edelstein and M. Genet, *Phys. Rev. B., 28,* 4923 (1983).

19 R. H. Banks and N. M. Edelstein, *J. Chem. Phys., 73,* 3589 (1980).

20 D. L. Wood, J. Ferguson, K. R. Knox and S. F. Dillon Jr., *J. Chem. Phys., 39,* 890 (1963).

21 K. Rajnak, E. Gamp, R. Shinomoto and N. Edelstein, *J. Chem. Phys.* in press.

22 A. Abragam and B. Bleaney, 'Electron Paramagnetic Resonance of Transition Ions', Oxford University Press, London, 1970.

23 K. Rajnak, R. H. Banks, E. Gamp and N. Edelstein, *J. Chem. Phys.* in press.

24 M. T. Hutchings, *Solid State Physics, 16,* 227 (1964).